scientific reports

Check for updates

OPEN

Chronic alcohol consumption downregulates TRPA1 ion channel and the main peptidergic messengers of the Edinger-Westphal nucleus

Ammar Al-Omari[1,2,9], Izabella Török[2,9], Balázs Zoltán Zsidó[2], Csaba Hetényi[2,4], Erika Pintér[2], Zoltán Sándor[2], Gergely Berta[3], Péter Szocsics[5,6], Péter Gombás[7], Tünde Biró-Sütő[2], Balázs Gaszner[8] & Viktória Kormos[2]✉

The urocortin 1 (UCN1) and cocaine- and amphetamine-regulated transcript (CART) co-expressing neurons of the centrally projecting Edinger-Westphal nucleus (EWcp), regulate the function of reward- and addiction-related brain areas. EWcp/UCN1/CART neurons highly express the transient receptor potential ankyrin 1 (TRPA1) cation channel. We hypothesized that alcohol and its metabolites may influence TRPA1 ion channels. We also anticipated that 3-months chronic limited-access voluntary alcohol consumption in mice affects EWcp/TRPA1 expression resulting in altered UCN1 and CART dynamics and alcohol consumption. Alcohol preference and serum amylase were assessed to validate the model. In the mouse EWcp, immunofluorescence targeting UCN1 and CART peptides were performed to assess neuronal activation as well as UCN1 and CART peptides content. Mouse *Trpa1*, *Cartpt*, and *Ucn1* as well as human *TRPA1* expression was semi-quantified by RNAscope in situ hybridization. In silico modelling and computational docking were performed to test the ability of alcohol and its metabolites to activate human TRPA1 channels. Alcohol preference gradually declined over the course of the study. Alcohol treatment significantly increased serum amylase level and proportionally decreased *Trpa1*, *Cartpt*, and *Ucn1* mRNA expression in the EWcp. Moreover, CART but not UCN1 peptide content was also reduced. We demonstrated *TRPA1* expression in the human EWcp/UCN1/CART neurons and provided translational evidence that alcohol and its metabolites activate the human TRPA1. We conclude that reduced EWcp/TRPA1 expression may may diminish alcohol preference offering novel potential therapeutic target.

Alcohol use disorder (AUD) is a serious public health problem that leads to more than 3 million deaths worldwide yearly. Consequences of AUD include mental and behavioral changes as well as mood disorders resulting in substantial socioeconomical implications[1,2].

The centrally projecting Edinger-Westphal nucleus (EWcp) neurons express several reward-, stress- and energy expenditure-related neuropeptides, e.g., cholecystokinin, pituitary adenylate cyclase-activating polypeptide and substance P[3,4], but the vast majority neurons co-express urocortin 1 (UCN1) and cocaine- and amphetamine-regulated transcript peptide (CART)[4–6].

Importantly, the EWcp UCN1/CART-expressing neurons project to reward and addiction-related brain areas including the ventral tegmental area (VTA), dorsal raphe nucleus (DRN), central nucleus of amygdala (CeA)

[1]Department of Cosmetic Science, Faculty of Allied Medical Sciences, Al-Ahliyya Amman University, Amman 19328, Jordan. [2]Department of Pharmacology and Pharmacotherapy, Medical School, University of Pécs, Szigeti út 12, Pecs 7624, Hungary. [3]Department of Medical Biology, Medical School, University of Pécs, Pecs 7624, Hungary. [4]National Laboratory for Drug Research and Development, Budapest, Hungary. [5]Human Brain Research Laboratory, HUN-REN Institute of Experimental Medicine, Budapest 1083, Hungary. [6]Szentágothai János Doctoral School of Neuroscience, Semmelweis University, Budapest 1085, Hungary. [7]Department of Pathology, St. Borbála Hospital, Tatabánya 2800, Hungary. [8]Department of Anatomy, Medical School and Research Group for Mood Disorders, Centre for Neuroscience, University of Pécs, Pecs 7624, Hungary. [9]Ammar Al-Omari and Izabella Török contributed equally to this work. ✉email: viktoria.kormos@aok.pte.hu

and the lateral septum (LS)[3]. All these brain regions express the receptors of UCN1, namely corticotropin-releasing hormone receptor type 1 and type 2 (CRH1R and CRH2R)[7]. Among these, the serotonergic DRN and the dopaminergic VTA play a crucial role in the development of alcohol abuse[8,9]. Despite that CART's precise physiological role remains unclear, largely due to the lack of well-defined, specific CART receptors[10], CART contributes to the regulation of alcohol consumption *via* the VTA, LH and CeA[11,12]. Moreover, the EWcp UCN1/CART neurons have recently been proven to play role in alcohol and substance-dependence related processes[3,7,13].

EWcp UCN1/CART neurons are extremely sensitive to alcohol[3]. They show a dose-dependent marked FOS (acute neuronal activation marker)[14–17] and FOSB (chronic neuronal activation marker)[18,19] response to acute and chronic, active and passive (self-administered) alcohol exposure. In line with that, high alcohol-preferring mice and rats express significantly higher level of *Ucn1* compared to low alcohol-preferring strains[20–23]. Moreover, electrolytic lesion of the EWcp dramatically reduced alcohol preference[24,25],.

Despite the large body of literature data on the role of CART in regulating addiction and reward behaviors[26,27], only few studies investigated the role of EWcp/CART. For instance, CART knockout (KO) mice exhibited lower alcohol preference than wild-type mice[28], moreover low alcohol-preferring DBA/2J mice show decreased CART mRNA and peptide expression in the EWcp compared to alcohol-preferring C57BL/6J mice[17]. The full UCN1/CART co-localization in the EWcp, along with their elevated levels in high alcohol preference mice implies a shared and significant role in controlling alcohol consumption and associated behaviors.

Transient receptor potential ankyrin 1 (TRPA1) is a non-selective cation channel primarily expressed by peripheral nociceptive neurons[29–31]. TRPA1 activation results in calcium influx, which can initiate several signaling processes[32], including neuropeptide release[33]. Only limited knowledge has been accumulated on its central role and to the best of our knowledge it has not been studied in relation to alcohol addiction. Some articles described the relationship between alcohol and TRPA1, but exclusively in context of pain: One study by patch clamp and calcium imaging reported that ethanol directly activates human TRPA1 expressed in human embryonic kidney-derived 293 (HEK293)[34]. Alcohol is metabolized by alcohol dehydrogenase and cytochrome P450 (CYP2E1) into acetaldehyde, which is then converted to acetic acid[35]. Importantly, both acetaldehyde and acetic acid can directly human TRPA1 on HEK293 cells, and mouse TRPA1-expressing trigeminal ganglion neurons[36,37]. Notably, acetaldehyde failed to activate other TRP ion channels in sensory neurons[36]. A recent study found that acetaldehyde contributes to ethanol-evoked periorbital mechanical allodynia in mice *via* TRPA1[38].

Our research group previously identified EWcp/UCN1/CART neurons as primary site of *Trpa1* mRNA expression in the mouse brain[39] and demonstrated that the absence of a functionally active TRPA1 influenced UCN1 content in the EWcp in mouse models of depression[39] and posttraumatic stress disorder[40]. Most recently, we proved the functional activity of EWcp /TRPA1 using patch clamp and demonstrated its role in regulating UCN1 but not CART in a mouse model of acute alcohol exposure[41].

In the present study we aimed at investigating the EWcp/UCN1/CART/TRPA1 neurons in a mouse model of chronic alcohol consumption.

Methods

Animals

Twelve-weeks-old male C57BL/6 mice were housed in the animal facility of the Department of Pharmacology and Pharmacotherapy, University of Pécs, in a room with controlled temperature and humidity, in standard polycarbonate cages (365 mm x 207 mm x 144 mm) at 12-hour light-dark cycles (lights on: 6 a.m.). Standard rodent food and tap water were provided *ad libitum*. Experiments were performed based on animal ethics permit (BA02/2000-25/2021) by the Animal Welfare Committee of the University of Pécs and the Scientific Ethics Council for Animal Experiments, in accordance with the ARRIVE guidelines and the directives established by the European Communities council in 1986, in conjunction with the Law of XXVIII in 1998 governing animal care and use in Hungary.

Post mortem human brian samples

Perfusion-fixed human brains tissues were obtained from the Human Brain Research Laboratory, HUN-REN Institute of Experimental Medicine (Budapest, Hungary). Three deceased subjects who died of extracranial disease and showed no signs of any neurological or mental disorders were used. From each brain, two representative sections of the EWcp were subjected to the qualitative morphological study. Perfusion, dissection, sectioning were performed as described earlier[42]. The study received ethical approval from the Regional and Institutional Committee of Science and Research Ethics of the Scientific Council of Health (ETT TUKEB 15032/2019/EKU) and was conducted in adherence to the principles of the Declaration of Helsinki.

Experimental design

Qualitative morphological and in-silico modelling studies

Representative EWcp sections from *post mortem* human brains were used to examine *TRPA1* expression in EWcp/UCN1/CART neurons.

In-silico modelling study was performed to examine the ability of ethanol and its metabolites acetaldehyde and acetic acid to bind to activate human TRPA1.

Semi-quantitative morphological examination of EWcp in chronic alcohol consumption model

Mice were assigned into control and treated groups ($n = 10$). After habituation to 2 drinking bottles in active dark period (18:00–06:00), the treated group received one bottle with tap water and one with alcohol diluted in tap water. For controls, both were filled with tap water. Mice were free to drink *ad libitum* according to their individual preference. During habituation, alcohol was gradually introduced, starting with a 5% concentration in the first and 7.5% in the second week. Subsequently, 10% alcohol was offered for the next three months for 12 h during the dark period. Mice were sacrificed in the early light phase after the last night of alcohol exposure. Eight mice per group were processed for histological studies.

Alcohol preference measurement

To assess alcohol preference, the water and alcohol consumption was measured every 2 weeks for 12 h in the active period (18:00–6:00). The alcohol preference was calculated according to the formula: [alcohol consumption (g) / (water consumption (g) + alcohol consumption (g))] x 100. The alcohol and water consumption was detected in groups to avoid the effect of social isolation on alcohol drinking[43].

Perfusion and tissue collection

Animals were euthanized by an intraperitoneal urethan (2.4 g/kg) injection in the between 8 am and 11 am. Mice were transcardially perfused, brains were dissected, postfixed, sectioned and stored as previously described[42]. Four representative EWcp sections (from Bregma – 2.92 to – 4.04[44] per animal were selected for each staining.

Serum amylase measurement

To validate our model, serum amylase levels were measured from blood samples collected during the prefusion, using an automated routine enzymatic colorimetric assay. The assay was performed at an accredited laboratory (Department of Laboratory Medicine, Medical School, University of Pécs, Hungary) utilizing the Cobas Pro c503 analyzer (Roche Diagnostics GmbH, Mannheim, Germany).

RNAscope in situ hybridization (ISH)

RNAscope ISH was performed to measure the expression of *Cartpt*, and *Ucn1* mRNA in EWcp. The pretreatment procedure was optimized for 30 µm-thick PFA-fixed Sect.[39]. Further steps (probe hybridization, signal amplification and channel development) were performed according to RNAscope Multiplex Fluorescent Reagent Kit v2 user manual (ACD, Hayward, CA, United States). Mouse *Cartpt* (ACD; Cat. No.: 432001) and *Ucn1* probes (ACD; Cat. No.: 466261) were visualized by cyanine 3 (Cy3) (1:3000 for *Cartpt*) and fluorescein (1:3000 for *Ucn1*) dyes, respectively. Counterstaining was performed by 4',6-diamidino-2-phenylindol (DAPI) (ACD). After washes, slides were covered with ProLong Gold Antifade (Thermo Fisher Scientific, Waltham, MA, USA; Cat. number: P10144) medium and stored at -20 °C until digitalization.

RNAscope ISH combined with Immunofluorescence

RNAscope ISH targeting mouse *Trpa1* and human *TRPA1*, combined with UCN1 immunofluorescence were performed on mouse and human EWcp samples to confirm the expression of *TRPA1* mRNA in human EWcp/UCN1neurons and to examine the effect of chronic alcohol consumption on *Trpa1* expression and UCN1 content in the mouse EWcp.

Samples were subjected to the RNAscope procedure as described above. Human *TRPA1* probe (ACD; Cat. number: 837411) and mouse *Trpa1* (ACD; Cat. number: 400211) were used and visualized by Cy3 (1:750). After the RNAscope procedure, slides were treated with polyclonal rabbit anti-UCN1 antibody (RRID: AB 2315527, Cat. No.: ab283503, Abcam) diluted to 1:5000, for 24 h at 24 °C. After 2 × 15 min washes, Alexa 488-conjugated donkey anti-rabbit secondary antibody (Jackson Immunoresearch Europe Ltd., Cambridgeshire, United Kingdom; Cat. No: 711-545-152, diluted to 1:500) was used for 3 h at 24 °C. Sections were counterstained with DAPI (ACD) and covered as described above.

Mouse (ACD; Cat. No: 320881) and human 3-plex (ACD; Cat. No: 320861) positive control probes specific to *Polr2a* mRNA (fluorescein), *Ppib* mRNA (Cy3) and *Ubc* mRNA (cyanine 5, Cy5) and 3-plex negative (ACD; Cat. No: 320871) control probes to bacterial *dabP* mRNA were tested on the murine and human EWcp. The 3-plex positive control probes gave well-detectable signal in the EWcp, while the negative control probes did not give any recognizable fluorescence (images not shown).

Immunofluorescence

Immunofluorescence targeting CART was performed to semi-quantify the peptide content. Sections were washed 2 × 15 min with 0.1 M phosphate-buffered saline (PBS), treated with 5% Triton X-100 (Sigma Chemical, Zwijndrecht, Netherlands) in PBS for 30 min and blocked with 2% normal donkey serum in PBS. Sections were incubated overnight in the primary antibody (anti-CART rabbit antibody (Phoenix H-003-62 (55–102)) in 1:10.000 dilution) at room temperature. After PBS washes, samples were incubated at room temperature for 3 h in mixture of secondary antibody (Cy3-conjugated donkey anti-rabbit (Jackson 711-165-152) in 1:500 dilution. After PBS washes samples were mounted on gelatinated slides, air-ried and cover-slipped with glycerol-PBS (1:1).

The specificity of the rabbit CART antibody (RRID: AB 2313614 Phoenix Europe GmbH, Karlsruhe, Germany) was tested earlier[45]. In this study, omission or replacement of primary and secondary antibodies by non-immune sera abolished labelling.

Microscopy, digital imaging and morphometry

Samples were digitalized by Olympus FluoView 1000 confocal microscope (Olympus Europe, Hamburg, Germany) in analogue mode with sequential scanning. The imaging was performed using 80 µm confocal aperture, 3.5 µm optical thickness, 1024 × 1024 pixel resolution and 60x objective. The excitation and emission spectra were chosen *via* built-in setting of the FluoView software (FV10-ASW; Version 0102, Olympus, Europe, Hamburg, Germany). DAPI is shown in blue, fluorescein and Alexa 488 in green, Cy3 in red and Cy5 in white. All imaging parameters were set and maintained unaltered for imaging of all groups to obtain reliable comparability of non-edited images in the morphomertry.

The *Trpa1* mRNA signals appeared as scattered, distinguishable fluorescent dots which were counted manually in 4–5 EWcp sections per animal. Signal puncta in, 5–10 UCN1/CART neurons per section were counted and these values were then averaged as described above.

The UCN1 and CART signals showed a confluent or cluster-like patterns both at mRNA and peptide level. As counting of individual fluorescent dots was not possible, the intensity of the fluorescence was measured by ImageJ software (version 1.42., NIH, Bethesda, MD) in 5–10 cell bodies using four non-edited images *per* animal. The region of interest was manually determined at cytoplasmic areas of neurons. The signal density was corrected for the background signal. The average of the specific signal density (SSD) of 5–10 neurons was determined in four sections per animal. The average of these four values represented the SSD value of one mouse. The SSD was expressed in arbitrary units (a.u.).

In silico modelling

Structural modelling and computational docking were performed to confirm the ability of alcohol and its metabolite to activate human TRPA1 cation channel.

Alcohol, acetaldehyde and acetic acid were built in the 2D sketcher of FITTED[46,47] saved as *.sdf* file and converted to *.mol2* file with the Convert function. Atomic charges were added, and rotatable bonds were identified with Smarts in the graphical user interface of FITTED.

The atomic coordinates of the human TRPA1 cation channel were used from our previous paper[48]. Briefly, the Protein Data Bank (PDB[49] structure with PDB code 6pqp[50] was used. Chain A was kept of the homotetramer structure, the missing residues were homology modelled with SWISS-MODEL[51] and the final resultant structure was energy minimized with GROMACS[48,52]. The FITTED built-in target preparatory steps were executed with default settings, in Prepare the protein is converted to a *.mol2* file, hydrogen atoms are added (if necessary), and the amino acid side chain conformations are optimized. In Process the binding site is identified (using the original ligand of PDB:6pqp).

The non-covalent and covalent functions of docking in FITTED were used with default settings. Covalent warhead was only recognized in the case of acetaldehyde, as expected. C621 was specified as the covalently binding amino acid. All three ligands were docked in non-covalent mode, as well. Five docking runs were carried out in each case. The results were ranked according to their calculated energy of binding, and only the most favorable rank was printed out as a *.sdf* file.

Statistics

Data from each experimental group were expressed as mean ± standard error of the mean. The datasets were tested for normality[53] and evaluated using Student *t* test. Pearson's and Spearman's rank tests was also applied to search for correlations. Analyses were performed using *Statistica 8.0* (StatSoft, Tulsa, OK) software (alpha = 5%).

Results

Model validation

Alcohol preference and serum amylase measurement were performed to confirm the alcohol consumption by mice and prove the model validity.

Alcohol preference was higher at the beginning of the experiment and showed a significant proportional decline throughout the experimental period (Fig. 1A). We found a significant negative correlation between alcohol preference and time in weeks ($p = 0.049$, Pearson's r=-0.881). Serum amylase levels were significantly higher in alcohol-treated mice compared to the controls (Student *t* test, $p = 0.002$; Fig. 1B).

EWcp response in the mouse model of chronic voluntary alcohol consumption

To assess neuromorphological changes in the EWcp in response to chronic alcohol consumption, RNAscope ISH targeting *Trpa1*, *Ucn1*, and *Cart* mRNA as well as immunofluorescence targeting UCN1 and CART peptide were performed.

Alcohol treatment significantly reduced the number of *Trpa1* transcripts in the EWcp/UCN1/CART neurons compared to controls (Student *t* test, $p = 0.0001$; Fig. 2A).

When assessing UCN1 mRNA and peptide, we found that alcohol treatment did not influence the UCN1 peptide content significantly (Student *t* test, $p = 0.59$; Fig. 2B). However, there was a significantly lower *Ucn1* mRNA expression in the treatment group compared to controls (Student *t* test, $p = 4.26 \times 10^{-6}$; Fig. 2C).

Alcohol-treated mice showed significantly lower CART peptide (Student *t* test, $p = 0.026480$; Fig. 2D) and *Cartpt* mRNA (Student *t* test, $p = 1.61 \times 10^{-4}$; Fig. 2E) content in the EWcp compared to the controls.

A multiple correlation analysis revealed positive correlations between the number of EWcp *Trpa1* transcripts and the *Ucn1* (Spearman's $\rho = 0.645$; $p = 0.0067$; Fig. 3A) as well as *Cartpt* (Spearman's $\rho = 0.91$; $p = 8.82 \times 10^{-7}$; Fig. 3B) mRNA expression, regardless of the treatment conditions. However, the number of *Trpa1* transcripts did not correlate with the UCN1 (Spearman's $\rho = 0.039$; $p = 0.89$; Fig. 3C) and CART (Spearman's $\rho = 0.46$; $p = 0.072$; Fig. 3D) peptide contents.

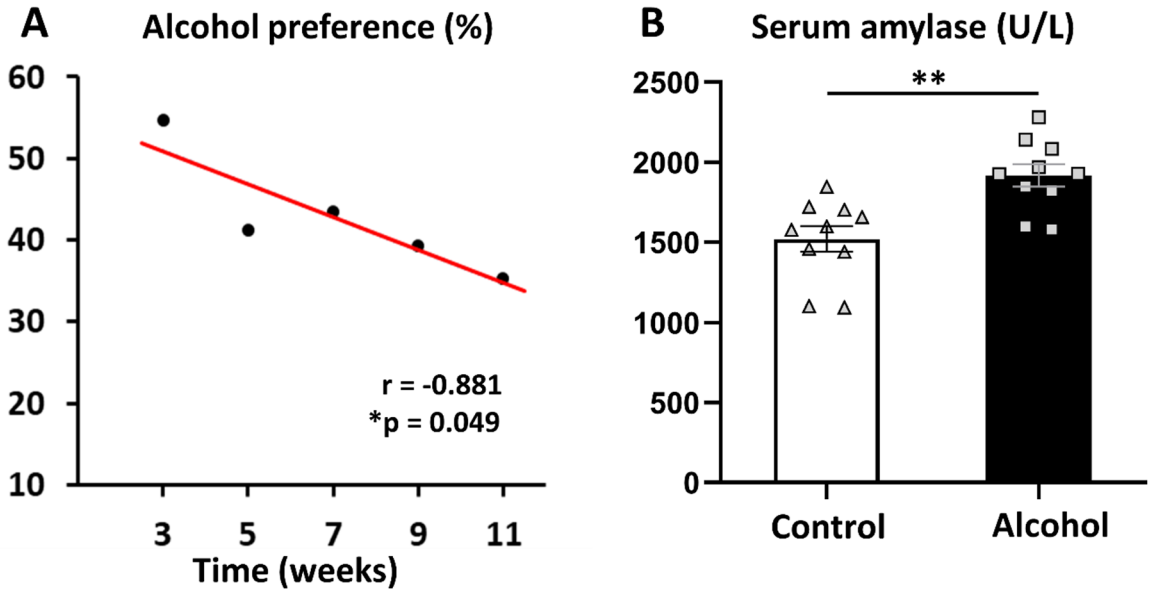

Fig. 1. Validation of the mouse model of chronic dark-phase voluntary alcohol consumption. (**A**) A significant negative correlation between alcohol preference and time in weeks, in a 3 months long mouse model of dark-phase voluntary (10%) alcohol (ethanol) consumption. ρ = Spearman's rank correlation coefficient. (**B**) Quantitative evaluation of amylase concentration in the serum of mice, after voluntary consumption of 10% alcohol in the dark phase for 3 months. Columns show means ± SEM of serum amylase concentration (U/L) ($n = 10$; $^{**}p = 0.001$; Student t test).

Human EWcp expresses alcohol sensitive *TRPA1* mRNA

To support the translational relevance of our study, we performed RNAscope ISH targeting human *TRPA1* combined with immunofluorescence both for UCN1 (Fig. 4A-B) and CART (Fig. 4C-D) on a human EWcp sections. Furthermore, the co-localization of *UCN1* and CART has been also shown in the human EWcp (Fig. 4E-G). Indeed, we confirmed the expression of *TRPA1* in the human EWcp/UCN1/CART positive neurons.

Moreover, we performed in silico modelling and computational docking study, to confirm the ability of alcohol and its metabolite to activate human TRPA1, and to test their possible mode of interaction with human TRPA1.

The docking of small ligands acetaldehyde, acetic acid and ethanol to the nucleophilic, agonist binding site of TPRA1 (Fig. 5A) was performed as previously[48]. The covalent binding mode of acetaldehyde (Fig. 5B), and the non-covalent binding modes of acetaldehyde, acetic acid and ethanol were produced (Fig. 5C-E). The ligands are binding to the intracellular region, in the nucleophilic, agonist binding site (Fig. 5A) characterized by three cysteine amino acids, of which C621 is the covalently binding[48,54]. Only acetaldehyde is capable of forming a covalent interaction with C621 through an aldehyde type of covalent bond (Fig. 5B). The calculated energy of binding of the covalently bound acetaldehyde is -56.92 kcal/mol, which is ca. three times higher compared to the non-covalent energy of binding of all three ligands, that are within the range of -16 to -21 kcal/mol. In the non-covalent binding mode acetaldehyde and acetic acid interact with the hydroxyl group of T684, and ethanol interacts with the backbone oxygen of Y662. The most favorable calculated energy of binding of acetaldehyde agrees well with experimental findings, that acetaldehyde is the strongest agonist out of the three investigated ligands.

Discussion

The UCN1/CART/EWcp neurons contribute to the regulation of alcohol consumption, through direct neuroanatomical connections to several alcohol and addiction-related brain areas including the VTA, CeA, DRN and LS[3,13,17,50]. High alcohol preference rodents exert elevated EWcp/UCN1 levels[21–23], whereas low alcohol preference is associated with low EWcp/CART mRNA and peptide levels[17]. Moreover, reduced alcohol intake and preference was observed in CART KO mice[28]. Furthermore, lesions of the rodent Edinger-Westphal nucleus greatly attenuate ethanol preference[24,25]. However, it is also important to highlight, that the ability of EWcp to the regulate alcohol consumption patterns is not limited to the peptidergic CART/UCN1 neurons, as the glutamatergic neurons may also contribute[56].

Our research group has previously proved the presence of functional TRPA1 ion channels murine EWcp/UCN1/CART neurons, contributing to modulation of UCN1 turnover in acute alcohol exposure. However, neither *Cartpt* mRNA nor CART peptide content was altered by acute alcohol treatment[41]. Based on the known role of CART in addiction[3,13,57], in the present study, we aimed to investigate the EWcp/UCN1/CART/TRPA1 in a mouse model of chronic voluntary alcohol consumption.

Numerous animal models exist for studying chronic alcohol exposure, each with limitations[58]. Based on our preliminary experiments testing various alcohol concentrations and protocols, we developed a voluntary

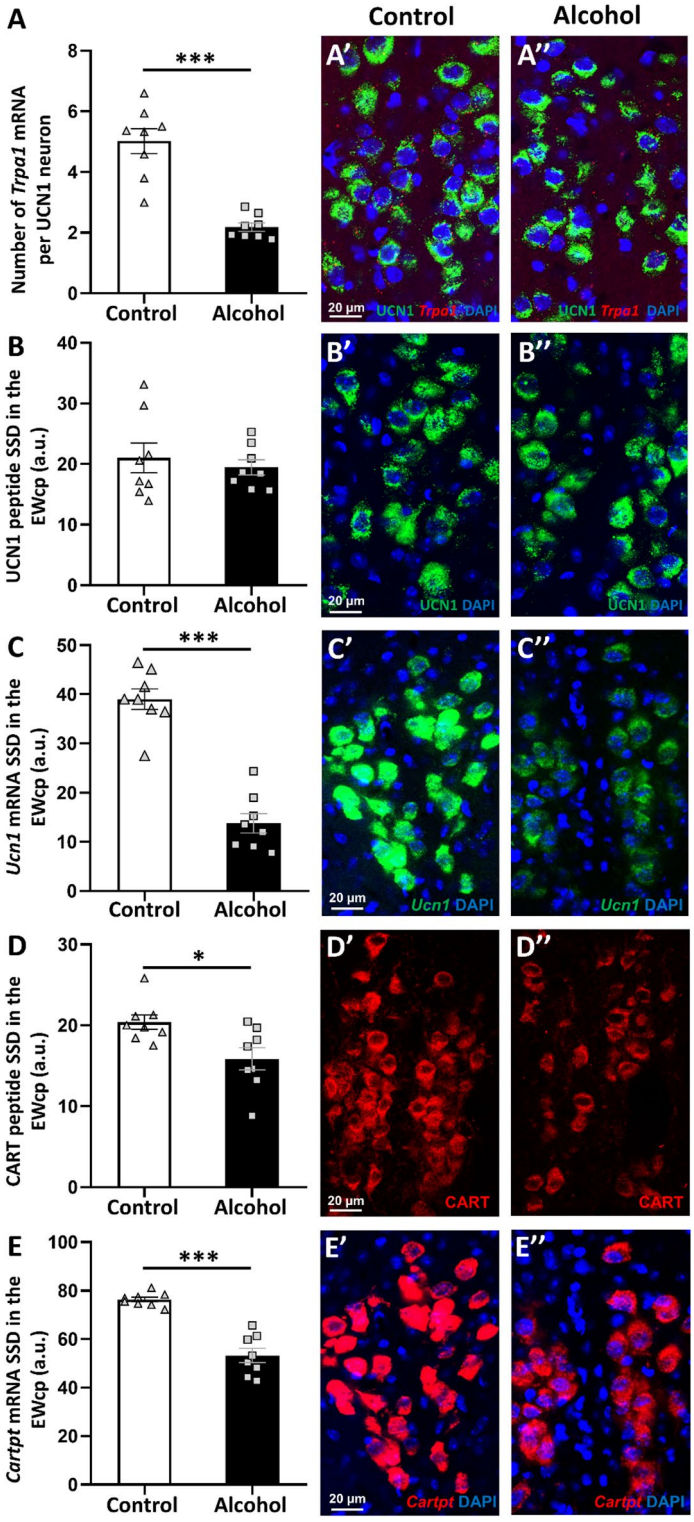

limited-access model. We found that mice willingly consumed a 10% ethanol solution without added sugar, gradually titrated from 5% over two weeks. This was important as mice often reduce intake of unsweetened alcohol[58]. Our results align with a study showing that C57BL/6J mice prefer unsweetened alcohol over water, with preference increasing up to 10% ethanol and declining at higher concentrations[59]. This was particularly important to avoid the known rewarding effect of sugar[60]. Moreover, to avoid the effect of social isolation on alcohol drinking patterns[61,62], mice were kept in their own cages, in groups with their littermates. Because AUD often develops within a decade or less after drinking initiation[63], we maintained the model for 3 months which corresponds to approximately 10 years in human[64].

At the beginning of the experiment, when the 10% alcohol concentration was offered to the mice, alcohol preference was 54.64% and continuously decreased with the time till 35.31% at the end of the experiment. Elevated serum amylase level in our treated mice supports the validity of our chronic alcohol consumption

◂**Fig. 2**. Response of the mouse centrally projecting Edinger–Westphal nucleus (EWcp) to chronic dark-phase voluntary alcohol consumption. (A) Columns show the number of transient receptor potential ankyrin 1 (*Trpa1)* mRNA transcripts in the urocortin 1 (UCN1)-expressing neurons of the mice EWcp, after voluntary consumption of alcohol (10% ethanol) in the dark phase for 3 months (n = 6; ***p = 0.0001; Student *t* test). (**A**′ and **A**″) Representative fluorescence images showing the expression of *Trpa1* mRNA (red) by RNAscope in situ hybridization and its co-localization with the UCN1 peptide (green) by immunofluorescence, in the EWcp of controls and alcohol-treated mice. (**B**) Columns show UCN1 peptide specific signal density (SSD) in the EWcp. (**B**′ and **B**″) Representative images illustrate UCN1 peptide (green) immunoreactivity in the EWcp in control and alcohol-treated mice. (**C**) Columns show *Ucn1* mRNA SSD in the EWcp ($n = 8$; $^{***}p = 4.26 \times 10^{-6}$; Student *t* test). (**C**′ and **C**″) Representative fluorescence images showing the expression of *Ucn1* mRNA (green) in the EWcp of control and alcohol-treated mice. (**D**) Columns show cocaine- and amphetamine regulated transcript (CART) peptide SSD in the EWcp ($n = 8$; $^{***}p = 0.026$; Student *t* test). (**D**′ and **D**″) Representative fluorescence images showing the CART peptide (red) in the EWcp of control and alcohol-treated mice. (**E**) Columns show *Cartpt* mRNA SSD in the EWcp ($n = 8$; $^{***}p = 1.61 \times 10^{-4}$; Student *t* test). (**E**′ and **E**″) Representative fluorescence images showing the expression of *Cartpt* mRNA peptide (red) in the EWcp of control and alcohol-treated mice. For nuclear counterstaining, 4′,6-diamidino-2-phenylindole (DAPI, blue) was used. a.u., arbitrary unit.

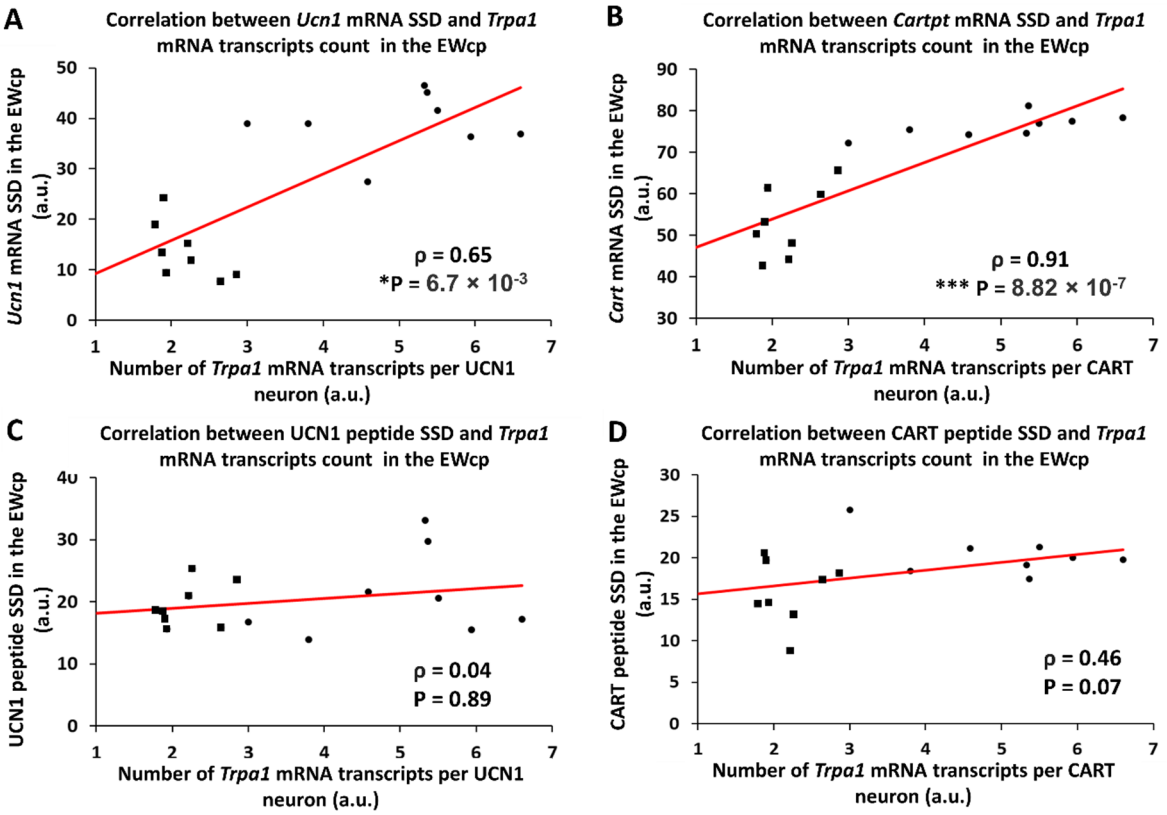

Fig. 3. Correlations between *Trpa1* mRNA transcripts count with urocortin 1 (UCN1) as well as cocaine- and amphetamine regulated transcript (CART) mRNA and peptides content in the centrally projecting Edinger–Westphal (EWcp) in mouse model of chronic alcohol consumption. A significant positive correlation was observed between *Trpa1* mRNA count and *Ucn1* mRNA (A) as well as *Cartpt* mRNA specific signal density (SSD) (B), after voluntary consumption of 10% alcohol or water (control) in the dark phase for 3 months, regardless of the treatment conditions ($n = 16$). No significant correlations were detected between *Trpa1* mRNA count and the UCN1 (C) as well as CART (D) peptide SSDs, in the EWcp, after voluntary consumption of 10% alcohol or water (control) in the dark phase for 3 months, regardless of the treatment conditions ($n = 16$). a.u.: arbitrary unit; ρ = Spearman's rank correlation coefficient. Data from control groups are represented by circles, while data from alcohol-treated groups are depicted by squares.

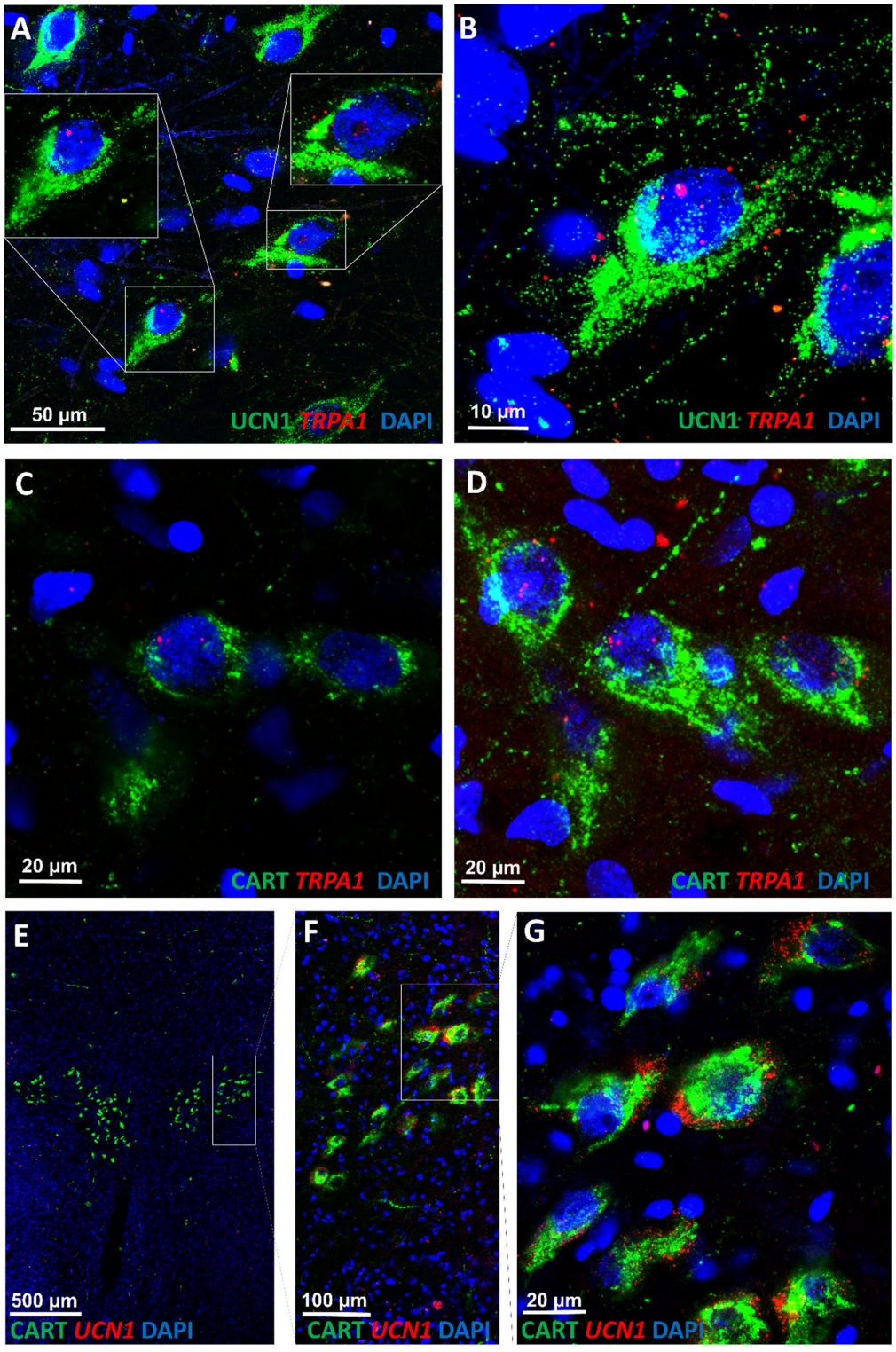

model[65–68]. Here we hypothesized that the reduction in alcohol preference over the time is attributed at least in part to the function of the EWcp/UCN1/CART neurons.

We found that chronic alcohol consumption significantly decreases *Trpa1* mRNA expression in EWcp/UCN1/CART neurons, consistently with acute alcohol exposure[41]. Alcohol and its metabolites, acetaldehyde and acetic acid pass the blood-brain barrier[69–71] act as TRPA1 agonists[34,36–38,72]. Repeated stimulation likely downregulated *Trpa1*, a common adaptive mechanism to sustained receptor activation[73] that may modulate the excitability and peptide turnover of EWcp/UCN1/CART neurons, potentially influencing alcohol consumption pattern.

We have previously demonstrated that acute alcohol treatment reduced EWcp/UCN1 peptide, but not mRNA[41]. However, when assessing EWcp/UCN1 dynamics in chronic alcohol consumption, we observed significant *Ucn1* downregulation whereas the peptide content did not change, suggesting disrupted UCN1

◀**Fig. 4**. Transient receptor potential ankyrin 1 (*TRPA1*) mRNA expression in the CART/UCN1 cells of the human centrally projecting Edinger-Westphal nucleus (EWcp). (**A**) Representative confocal image shows the expression of *TRPA1* mRNA (red) and its co-localization with the urocortin 1 (UCN1) peptide (green) in the human EWcp. (**B**) A Z projection of 18 confocal frames showing the left boxed cell in (**A**). (**C**) Representative confocal image of two CART-immunoreactive (green) cells in the human EWcp that express *TRPA1* mRNA (red). (**D**) Z projection of confocal images taken in the area shown in (**C**). (**E**) Low power magnification representative confocal image of the human EWcp area in the ventral periaqueductal gray upon CART immunofluorescence (green) and RNAscope in situ hybridization for *UCN1* mRNA (red). (**F**) The boxed area of the peptidergic cells in (**E**) is depicted in higher magnification. (**G**) A group of cells boxed in F is shown in a high power magnification confocal image. Note, that all CART immunorective (green) cells also contain *UCN1* mRNA, confirming their co-expression in the human EWcp. Nuclear counterstaining was performed with 4′,6-diamidino-2-phenylindole (DAPI, blue in all panels).

turnover. TRPA1 activation is known to induce peptide release from neurons[74–77]. We therefore propose that downregulation of *Trpa1* inhibits UCN1 peptide release from EWcp neurons, which in turn leads to a decrease in *Ucn1* mRNA expression through negative feedback[78–80]. Similarly, chronic alcohol treatment significantly reduced *Cartpt* mRNA expression in the EWcp, with a limited reduction in CART peptide content. This is consistent with a study showing that chronic maternal ethanol exposure decreases CART expression in the developing and adult offspring[81]. We also found a significant positive correlation between *Trpa1* transcripts count with the *Ucn1* and *Cartpt* mRNA levels, regardless the treatment conditions, further supporting a role for TRPA1 in regulating UCN1 and CART turnover[82].The observed differences in the dynamics of UCN1 and CART despite their co-localization may suggest peptide-specific regulatory influence of TRPA1 however, further research is needed to unveil such mechanisms.

The modulation of UCN1 and CART turnover *via* TRPA1-dependent mechanisms by alcohol and its metabolites in the EWcp, may in turn influence the function of alcohol-sensitive and reward-related downstream brain areas (VTA, CeA, DRN and LS) ultimately shaping alcohol consumption patterns[3,7,13].This is supported by the continuous decline in alcohol preference over the time associated with a lower *Ucn1* and *Cartpt* levels. This is in agreement with several studies showing reduced EWcp *Ucn1* and *Cartpt* in low alcohol preference rodent strai ns[17,21–23,28,83]. More recently, Pearl et al. (2025) demonstrated that inhibiting EW/CART neurons reduces alcohol intake, further underscoring their role in alcohol consumption regulation[84].The alcohol-induced response in EWcp was postulated to be a result of signaling *via* GABA-A receptors, modified by α2A/D-adrenoceptors and dopamine receptors[20], we propose that TRPA1 may also contribute[41].

The translational relevance of the present findings was supported by showing *TRPA1* mRNA in human EWcp in both UCN1 and CART-immunoreactive neurons, furthermore, using ultrasensitive RNAscope ISH technique combined with immunofluorescence we provided evidence that in line with mice[3], *UCN1* and CART are co-localized in the human EWcp also. Moreover, using in silico modelling and computational docking techniques further confirmed that alcohol and its metabolites bind to and activate human TRPA1.

There is no study without limitations. Because EWcp/UCN1/CART neurons express estrogen receptor beta and estrus cycle-related hormonal fluctuations modulate UCN1 levels, we recruited exclusively male mice in our study[85,86]. Because, as of today, no reliable TRPA1 antibody is available[87,88], we were unable to support our findings at protein level. In vivo pharmacological manipulation of TRPA1 was not feasible due to the lack of information on the safety and pharmacokinetic profiles of selective agonists and antagonists[89].

With respect to the limitations, we conclude that the progressive reduction in alcohol preference during chronic voluntary alcohol consumption is associated with a significant and proportional decrease in *Trpa1*, *Ucn1*, and *Cartpt* mRNA expression in the EWcp, with reduction inCART but not UCN1 peptides content. Hence, we propose that the alcohol-induced downregulation of EWcp/*Trpa1* inhibits both UCN1, and to a lesser extent, CART release. This ultimately modulates through several downstream alcohol-sensitive and reward-related brain areas the alcohol preference. We also proved that *TRPA1* is expressed in the human EWcp/UCN1/CART neurons, and that alcohol and its metabolites can directly activate human TRPA1. These findings suggest that EWcp/TRPA1 may regulate alcohol consumption behavior also in the human. Pharmacological intervention at TRPA1 may therefore represent a promising therapeutic strategy for AUD.

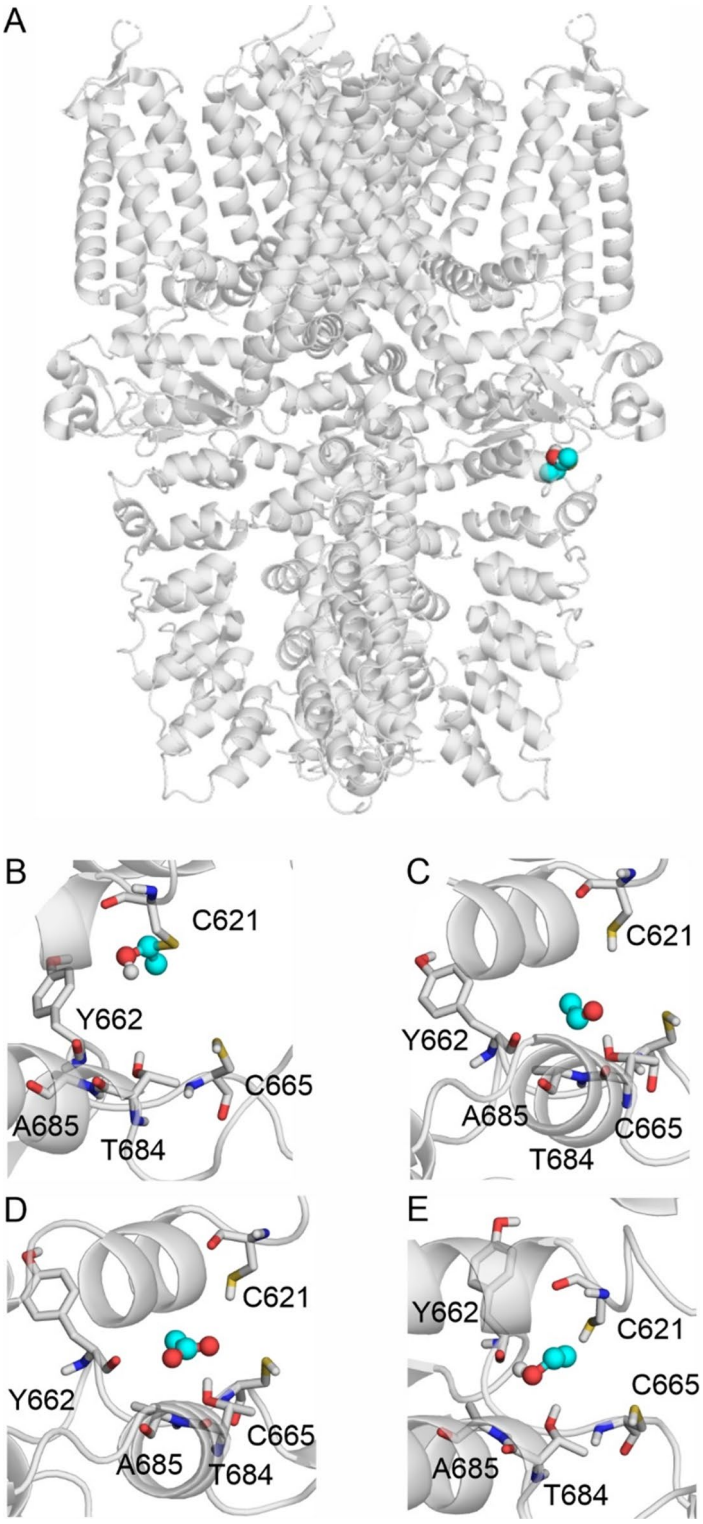

Fig. 5. Molecular interactions of alcohol and its metabolite with the human transient receptor potential ankyrin 1 (TRPA1) cation channel. (**A**) The human TRPA1 cation channel (grey cartoon) in complex with acetaldehyde (teal spheres) in the nucleophilic, agonist binding site. (**B**) A close-up of acetaldehyde covalently binding to C621 in the nucleophilic, agonist binding site. (**C**–**E**) The close-up of the non-covalent binding modes of acetaldehyde, acetic acid, and ethanol, respectively. The binding modes are shown as teal all atom representation balls and sticks, interacting amino acids are shown as grey sticks and labeled accordingly to PDB:6pqp, the rest of the binding site is shown as grey cartoon.

Data availability

The datasets used and/or analyzed during the current study are available from the corresponding author on reasonable request.

Received: 7 September 2025; Accepted: 10 December 2025
Published online: 12 December 2025

References

1. World Health Organization. Over 3 million annual deaths due to alcohol and drug use, majority among men. https://www.who.int/news/item/25-06-2024-over-3-million-annual-deaths-due-to-alcohol-and-drug-use-majority-among-men (Accessed 30 Aug 2025) (2024).
2. Martínez-Maldonado, A. et al. Effect of chronic alcohol consumption on brain structure in males with alcohol use disorder without a familiar history of alcoholism. *J. Psychiatr Res.* **149**, 210–216 (2022).
3. Zuniga, A. & Ryabinin, A. E. Involvement of centrally projecting Edinger-Westphal nucleus neuropeptides in actions of addictive drugs. *Brain Sci.* **10**(2), 67 (2020).
4. Priest, M. F. et al. Peptidergic and functional delineation of the Edinger-Westphal nucleus. *Cell. Rep.* **42**(8), 112992 (2023).
5. Kozicz, T. Neurons colocalizing urocortin and cocaine and amphetamine-regulated transcript immunoreactivities are induced by acute lipopolysaccharide stress in the Edinger-Westphal nucleus in the rat. *Neuroscience* **116**(2), 315–320 (2003).
6. Li, J. & Ryabinin, A. E. Oxytocin receptors in the mouse centrally-projecting Edinger-Westphal nucleus and their potential functional significance for thermoregulation. *Neuroscience* **498**, 93–104 (2022).
7. Schreiber, A. L. & Gilpin, N. W. Corticotropin-releasing factor (CRF) neurocircuitry and neuropharmacology in alcohol drinking. *Handb. Exp. Pharmacol.* **248**, 435–471 (2018).
8. Lowery-Gionta, E. G., Marcinkiewcz, C. A. & Kash, T. L. Functional alterations in the dorsal Raphe nucleus following acute and chronic ethanol exposure. *Neuropsychopharmacology* **40**(3), 590–600 (2015).
9. You, C., Vandegrift, B. & Brodie, M. S. Ethanol actions on the ventral tegmental area: novel potential targets on reward pathway neurons. *Psychopharmacol. (Berl).* **235**(6), 1711–1726 (2018).
10. Lau, J. & Herzog, H. CART in the regulation of appetite and energy homeostasis. *Front. Neurosci.* **8**, 313 (2014).
11. Ahmadian-Moghadam, H., Sadat-Shirazi, M. S. & Zarrindast, M. R. Cocaine- and amphetamine-regulated transcript (CART): A multifaceted neuropeptide. *Peptides* **110**, 56–77 (2018).
12. Maddern, X. J. et al. Cocaine and amphetamine regulated transcript (CART) mediates sex differences in binge drinking through central taste circuits. *Neuropsychopharmacology* **49**(3), 541–550 (2024).
13. Ong, Z. Y. & McNally, G. P. CART in energy balance and drug addiction: current insights and mechanisms. *Brain Res.* **1740**, 146852 (2020).
14. Ryabinin, A. E., Bachtell, R. K., Freeman, P. & Risinger, F. O. ITF expression in mouse brain during acquisition of alcohol self-administration. *Brain Res.* **890**(1), 192–195 (2001).
15. Weitemier, A. Z., Woerner, A., Bäckström, P., Hyytiä, P. & Ryabinin, A. E. Expression of c-Fos in Alko alcohol rats responding for ethanol in an operant paradigm. *Alcohol Clin. Exp. Res.* **25**(5), 704–710 (2001).
16. Sharpe, A. L., Tsivkovskaia, N. O. & Ryabinin, A. E. Ataxia and c-Fos expression in mice drinking ethanol in a limited access session. *Alcohol Clin. Exp. Res.* **29**(8), 1419–1426 (2005).
17. Giardino, W. J. et al. Control of chronic excessive alcohol drinking by genetic manipulation of the Edinger-Westphal nucleus urocortin-1 neuropeptide system. *Transl Psychiatry*. **7**(1), e1021 (2017).
18. Bachtell, R. K., Wang, Y. M., Freeman, P., Risinger, F. O. & Ryabinin, A. E. Alcohol drinking produces brain region-selective changes in expression of inducible transcription factors. *Brain Res.* **847**(2), 157–165 (1999).
19. Ozburn, A. R. et al. Chronic self-administration of alcohol results in elevated ΔFosB: comparison of hybrid mice with distinct drinking patterns. *BMC Neurosci.* **13**, 130 (2012).
20. Bachtell, R. K., Tsivkovskaia, N. O. & Ryabinin, A. E. Strain differences in urocortin expression in the Edinger-Westphal nucleus and its relation to alcohol-induced hypothermia. *Neuroscience* **113**(2), 421–434 (2002).
21. Bachtell, R. K. et al. The Edinger-Westphal-lateral septum urocortin pathway and its relationship to alcohol consumption. *J. Neurosci.* **23**(6), 2477–2487 (2003).
22. Fonareva, I. et al. Increased perioculomotor urocortin 1 immunoreactivity in genetically selected alcohol preferring rats. *Alcohol Clin. Exp. Res.* **33**(11), 1956–1965 (2009).
23. Turek, V. F. et al. Urocortin 1 expression in five pairs of rat lines selectively bred for differences in alcohol drinking. *Psychopharmacol. (Berl).* **181**(3), 511–517 (2005).
24. Bachtell, R. K., Weitemier, A. Z. & Ryabinin, A. E. Lesions of the Edinger-Westphal nucleus in C57BL/6J mice disrupt ethanol-induced hypothermia and ethanol consumption. *Eur. J. Neurosci.* **20**(6), 1613–1623 (2004).
25. Ryabinin, A. E. & Weitemier, A. Z. The urocortin 1 neurocircuit: ethanol-sensitivity and potential involvement in alcohol consumption. *Brain Res. Rev.* **52**(2), 368–380 (2006).
26. Bakhtazad, A., Vousooghi, N., Garmabi, B. & Zarrindast, M. R. CART peptide and opioid addiction: expression changes in male rat brain. *Neuroscience* **325**, 63–73 (2016).
27. Kuhar, M. J. CART peptides and drugs of abuse: A review of recent progress. *J. Drug Alcohol Res.* **5**, 235984 (2016).
28. Salinas, A. G., Nguyen, C. T., Ahmadi-Tehrani, D. & Morrisett, R. A. Reduced ethanol consumption and preference in cocaine- and amphetamine-regulated transcript (CART) knockout mice. *Addict. Biol.* **19**(2), 175–184 (2014).
29. Kádková, A., Synytsya, V., Krusek, J., Zímová, L. & Vlachová, V. Molecular basis of TRPA1 regulation in nociceptive neurons. A review. *Physiol. Res.* **66**(3), 425–439 (2017).
30. Meents, J. E., Ciotu, C. I. & Fischer, M. J. M. TRPA1: a molecular view. *J. Neurophysiol.* **121**(2), 427–443 (2019).
31. Talavera, K. et al. Mammalian transient receptor potential TRPA1 channels: from structure to disease. *Physiol. Rev.* **100**(2), 725–803 (2020).
32. Song, F. & Guo, J. Progress on structural biology of voltage-gated ion channels. *Zhejiang Da Xue Xue Bao Yi Xue Ban.* **48**(1), 25–33 (2019).
33. Anqueira-González, A. et al. Transcriptional correlates of chronic alcohol neuroadaptation in drosophila larvae. *Front. Behav. Neurosci.* **15**, 768694 (2021).
34. Komatsu, T., Uchida, K., Fujita, F., Zhou, Y. & Tominaga, M. Primary alcohols activate human TRPA1 channel in a carbon chain length-dependent manner. *Pflugers Arch.* **463**(4), 549–559 (2012).
35. Cederbaum, A. I. Alcohol metabolism. *Clin. Liver Dis.* **16**(4), 667–685 (2012).
36. Bang, S., Kim, K. Y., Yoo, S., Kim, Y. G. & Hwang, S. W. Transient receptor potential A1 mediates acetaldehyde-evoked pain sensation. *Eur. J. Neurosci.* **26**(9), 2516–2523 (2007).
37. Wang, Y. Y., Chang, R. B., Allgood, S. D., Silver, W. L. & Liman, E. R. A TRPA1-dependent mechanism for the pungent sensation of weak acids. *J. Gen. Physiol.* **137**(6), 493–505 (2011).
38. Landini, L. et al. Acetaldehyde via CGRP receptor and TRPA1 in Schwann cells mediates ethanol-evoked periorbital mechanical allodynia in mice: relevance for migraine. *J. Biomed. Sci.* **30**(1), 28 (2023).

39. Kormos, V. et al. Peptidergic neurons of the Edinger-Westphal nucleus express TRPA1 ion channel that is downregulated both upon chronic variable mild stress in male mice and in humans who died by suicide. *J. Psychiatry Neurosci.* **47**(3), E162–E175 (2022).
40. Konkoly, J. et al. Transient receptor potential Ankyrin 1 ion channel expressed by the Edinger-Westphal nucleus contributes to stress adaptation in murine model of posttraumatic stress disorder. *Front. Cell. Dev. Biol.* **10**, 1059073 (2022).
41. Al-Omari, A. et al. Functionally active TRPA1 ion channel is downregulated in peptidergic neurons of the Edinger-Westphal nucleus upon acute alcohol exposure. *Front. Cell. Dev. Biol.* **10**, 1046559 (2023).
42. Al-Omari, A. et al. Neuroanatomical evidence and a mouse calcitonin gene-related peptide model in line with human functional magnetic resonance imaging data support the involvement of peptidergic Edinger-Westphal nucleus in migraine. *Pain* **165**(12), 2774–2793 (2024).
43. Cullins, E. C. & Chester, J. A. Adolescent social isolation increases binge-like alcohol drinking in male but not female high-alcohol-preferring mice. *Alcohol Alcohol.* **59**(2), agae006 (2024).
44. Paxinos and Franklin. *The Mouse Brain in Stereotaxic Coordinates*. ISBN 0-12-547636-1. (Academic Press, 2001).
45. Armbruszt, S., Figler, M. & Ábrahám, H. Stability of CART peptide expression in the nucleus accumbens in aging. *Acta Biol. Hung.* **66**(1), 1–13 (2015).
46. Corbeil, C. R., Englebienne, P. & Moitessier, N. Docking ligands into flexible and solvated macromolecules. 1. Development and validation of FITTED 1.0. *J. Chem. Inf. Model.* **47**(2), 435–449 (2007).
47. Therrien, E. et al. Docking ligands into flexible and solvated macromolecules. 7. Impact of protein flexibility and water molecules on docking-based virtual screening accuracy. *J. Chem. Inf. Model.* **54**(11), 3198–3210 (2014).
48. Zsidó, B. Z., Börzsei, R., Pintér, E. & Hetényi, C. Prerequisite binding modes determine the dynamics of action of covalent agonists of ion channel TRPA1. *Pharmaceuticals (Basel).* **14**(10), 988 (2021).
49. Berman, H. M. et al. The protein data bank. *Nucleic Acids Res.* **28**(1), 235–242 (2000).
50. Suo, Y. et al. Structural insights into electrophile irritant sensing by the human TRPA1 channel. *Neuron* **105**(5), 882–894e5 (2020).
51. Waterhouse, A. et al. SWISS-MODEL: homology modelling of protein structures and complexes. *Nucleic Acids Res.* **46**(W1), W296–W303 (2018).
52. Van Der Spoel, D. et al. GROMACS: fast, flexible, and free. *J. Comput. Chem.* **26**(16), 1701–1718 (2005).
53. Shapiro, S. S. & Wilk, M. B. An analysis of variance test for normality. *Biometrika* **52**, 591–599 (1965).
54. Nemes, B. et al. Elucidation of the binding mode of organic polysulfides on the human TRPA1 receptor. *Front. Physiol.* **14**, 1180896 (2023).
55. Bluett, R. J., Yu, Y., Pauli, J. L., Campos, C. A. & Palmiter, R. D. Edinger-Westphal Urocortin-1 neurons regulate consumption and affect. *Cell. Rep.* **44**(6), 115814 (2025).
56. Zuniga, A., Smith, M. L., Caruso, M. & Ryabinin, A. E. Vesicular glutamate transporter 2-containing neurons of the centrally-projecting Edinger-Westphal nucleus regulate alcohol drinking and body temperature. *Neuropharmacology* **200**, 108795. https://doi.org/10.1016/j.neuropharm.2021.108795 (2021).
57. Vicentic, A. & Jones, D. C. The CART (cocaine- and amphetamine-regulated transcript) system in appetite and drug addiction. *J. Pharmacol. Exp. Ther.* **320**(2), 499–506 (2007).
58. Nieto, S. J., Grodin, E. N., Aguirre, C. G., Izquierdo, A. & Ray, L. A. Translational opportunities in animal and human models to study alcohol use disorder. *Transl Psychiatry*. **11**(1), 496 (2021).
59. Bachmanov, A. A., Tordoff, M. G. & Beauchamp, G. K. Ethanol consumption and taste preferences in C57BL/6ByJ and 129/J mice. *Alcohol Clin. Exp. Res.* **20**(2), 201–206 (1996).
60. Le, Q. et al. Binge-like sucrose self-administration experience inhibits cocaine and sucrose seeking behavior in offspring. *Front. Behav. Neurosci.* **11**, 184 (2017).
61. Moench, K. M. & Logrip, M. L. Housing condition differentially impacts escalation of alcohol Intake, relapse-like drinking, anxiety-like behavior, and stress history effects by sex. *Alcohol Clin. Exp. Res.* **45**(2), 480–489 (2021).
62. Miczek, K. A., DiLeo, A., Newman, E. L., Akdilek, N. & Covington, H. E. III. Neurobiological bases of alcohol consumption after social stress. *Curr. Top. Behav. Neurosci.* **54**, 245–281 (2022).
63. Hingson, R. W., Heeren, T. & Winter, M. R. Age at drinking onset and alcohol dependence: age at onset, duration, and severity. *Arch. Pediatr. Adolesc. Med.* **160**(7), 739–746 (2006).
6. Dutta, S. & Sengupta, P. Men and mice: relating their ages. *Life Sci.* **152**, 244–248 (2016).
65. D.Moulali. A study on gamma Glutamyl transferase and amylase levels in chronic alcoholics with hepatitis. *Int. J. Sci. Res. Publications*. **5**(Issue 11), 2250–3153 (2015).
66. Mehra, S. et al. Urolithin A attenuates severity of chronic pancreatitis associated with continued alcohol intake by inhibiting PI3K/AKT/mTOR signaling. *Am. J. Physiol. Gastrointest. Liver Physiol.* **323**(4), G375–G386. https://doi.org/10.1152/ajpgi.00159.2022 (2022).
67. Srinivasan, M. P. et al. Exposure to binge ethanol and fatty acid ethyl esters exacerbates chronic ethanol-induced pancreatic injury in hepatic alcohol dehydrogenase-deficient deer mice. *Am. J. Physiol. Gastrointest. Liver Physiol.* **322**(3), G327–G345. https://doi.org/10.1152/ajpgi.00263.2021 (2022).
68. Klöppel, G. & Zamboni, G. Acute and chronic alcoholic pancreatitis, including paraduodenal pancreatitis. *Arch. Pathol. Lab. Med.* **147**(3), 294–303. https://doi.org/10.5858/arpa.2022-0202-RA (2023).
69. Nurmi, M., Kiianmaa, K. & Sinclair, J. D. Brain ethanol levels after voluntary ethanol drinking in AA and Wistar rats. *Alcohol* **19**(2), 113–118 (1999).
70. Quertemont, E. & Tambour, S. Is ethanol a pro-drug? The role of acetaldehyde in the central effects of ethanol. *Trends Pharmacol. Sci.* **25**(3), 130–134 (2004).
71. Wang, J. et al. Oxidation of ethanol in the rat brain and effects associated with chronic ethanol exposure. *Proc. Natl. Acad. Sci. U S A.* **110**(35), 14444–14449 (2013).
72. De Logu, F. et al. Schwann cells expressing nociceptive channel TRPA1 orchestrate ethanol-evoked neuropathic pain in mice. *J. Clin. Invest.* **129**(12), 5424–5441 (2019).
73. Finch, A. R., Caunt, C. J., Armstrong, S. P. & McArdle, C. A. Agonist-induced internalization and downregulation of gonadotropin-releasing hormone receptors. *Am. J. Physiol. Cell. Physiol.* **297**(3), C591–C600 (2009).
74. Nassini, R. et al. Transient receptor potential ankyrin 1 channel localized to non-neuronal airway cells promotes non-neurogenic inflammation. *PLoS One*. **7**(8), e42454 (2012).
75. Julius, D. TRP channels and pain. *Annu. Rev. Cell. Dev. Biol.* **29**, 355–384 (2013).
76. Shatillo, A. et al. Cortical spreading depression induces oxidative stress in the trigeminal nociceptive system. *Neuroscience* **253**, 341–349 (2013).
77. Dussor, G. et al. Targeting TRP channels for novel migraine therapeutics. *ACS Chem. Neurosci.* **5**(11), 1085–1096 (2014).
78. Liu, J., Kahri, A., Teppo, A. M. & Voutilainen, R. Regulation of parathyroid hormone gene expression and peptide secretion in human parathyroid cells. *Eur. J. Endocrinol.* **130**(4), 394–401 (1994).
79. Bustin, S. Molecular biology of the Cell, sixth edition; ISBN: 9780815344643; and molecular biology of the cell, sixth edition, the problems book; ISBN 9780815344537. *Int. J. Mol. Sci.* **16**(12), 28123–28125 (2015).
80. Chappleboim, A., Joseph-Strauss, D., Gershon, O. & Friedman, N. Transcription feedback dynamics in the wake of cytoplasmic mRNA degradation shutdown. *Nucleic Acids Res.* **50**(10), 5864–5880 (2022).

81. Dandekar, M. P., Bharne, A. P., Borkar, P. D., Subhedar, N. K. & Kokare, D. M. Maternal ethanol exposure reshapes CART system in the rat brain: correlation with development of anxiety, depression and memory deficits. *Neuroscience* **406**, 126–139 (2019).
82. Al-Omari, A. et al. TRPA1 modulates urocortin 1 turnover in the centrally projecting Edinger-Westphal nucleus in a CGRP-induced migraine model. *Neuropharmacology*. 110753 https://doi.org/10.1016/j.neuropharm.2025.110753 (2025).
83. Ryabinin, A. E. et al. Urocortins: crf's siblings and their potential role in anxiety, depression and alcohol drinking behavior. *Alcohol* **46**(4), 349–357 (2012).
84. Pearl, A. J. et al. Midbrain ghrelin receptor signalling regulates binge drinking in a sex specific manner. *Nat. Commun.* **16**(1), 2568. https://doi.org/10.1038/s41467-025-57880-w (2025).
85. Derks, N. M., Roubos, E. W. & Kozicz, T. Presence of estrogen receptor beta in urocortin 1-neurons in the mouse non-preganglionic Edinger-Westphal nucleus. *Gen. Comp. Endocrinol.* **153**(1–3), 228–234 (2007).
86. Derks, N. M., Gaszner, B., Roubos, E. W. & Kozicz, L. T. Sex differences in urocortin 1 dynamics in the non-preganglionic Edinger-Westphal nucleus of the rat. *Neurosci. Res.* **66**(1), 117–123 (2010).
87. Virk, H. S. et al. Validation of antibodies for the specific detection of human TRPA1. *Sci. Rep.* **9**(1), 18500 (2019).
88. Rojas-Galvan, N. S., Ciotu, C. I., Heber, S. & Fischer, M. J. M. Correlation of TRPA1 RNAscope and agonist responses. *J. Histochem. Cytochem.* **72**(5), 275–287 (2024).
89. Broad, L. M. et al. Preclinical and clinical evaluation of a novel TRPA1 antagonist LY3526318. *Pain* **166**(8), 1893–1908 (2025).

Acknowledgements

We acknowledge the Digital Government Development and Project Management Ltd. for awarding us access to the Komondor HPC facility based in Hungary. Authors are grateful for the Reviewers and Editors of the Journal for their thorough work and valuable suggestions.

Author contributions

VK planned the study. VK, AA and IT accomplished the animal experiments. VK, AA, IT and TBS performed the immunostainings and *in situ* hybridizations. ZS contributed to data acquisition. AA, IT and VK carried out the morphometry, cell counting and statistical evaluations. BG and GB helped with microscopy and digital images. EP provided the C57BL/6 mice. CsH and BZZs performed the *in silico* studies. PSz and PG was responsible for collection of the perfused human EW samples. AA and VK prepared the figures and wrote the manuscript. All authors have read and approved the final version of the manuscript.

Funding

This work was supported by the the Research grant of Medical School, University of Pécs (KA-2022-29; 008_2025_PTE_RK/36) and by the János Bolyai Research Scholarship of the Hungarian Academy of Sciences (BO/00750/22/5) to VK. BG and EP was supported by the Thematic Excellence Program 2021 Health Sub-program of the Ministry for Innovation and Technology in Hungary, within the framework of the EGA-16 project of Pécs University (TKP2021-EGA-16); and BG by the grant NKFI-146117. BZZs was supported by the János Bolyai Research Scholarship of the Hungarian Academy of Sciences (BO/00189/24/5). CsH and EP were supported by the National Research, Development and Innovation Office (PharmaLab, RRF-2.3.1-21-2022-00015) and EP by the Hungarian Brain Research Program (NAP 3) HUNREN.

Declarations

Competing interests

The authors declare no competing interests.

Additional information

Correspondence and requests for materials should be addressed to V.K.